Journal of Applied Polymer Science

Replication of laser-textured alumina surfaces by polydimethylsiloxane: Improvement of surface hydrophobicity

Bekir Sami Yilbas,[1,2] M. Rizwan Yousaf,[2] H. Ali,[2] N. Al-Aqeeli[2]
[1]Center of Research Excellence in Renewable Energy, KFUPM, Dhahran, 31261, Saudi Arabia
[2]ME Department, KFUPM, Dhahran, 31261, Saudi Arabia
Correspondence to: B. S. Yilbas (E-mail: bsyilbas@kfupm.edu.sa)

ABSTRACT: Alumina tiles are textured by a laser beam to obtain improved hydrophobic characteristics at the surfaces. Since the textured surfaces are optically opaque, the resulting surfaces are copied and replicated by polydimethylsiloxane (PDMS). Some of the texture features such as whiskers-like structures with complex shapes could not be copied by PDMS and synthesized silica particles are deposited onto PDMS copied and replicated surfaces to create a lotus effect. Analytical tools are incorporated to characterize the PDMS copied and replicated surfaces as well as synthesized silica particles deposited surfaces. Dynamic water contact angle measurements are carried out to assess hydrophobic characteristics of the resulting surfaces. It is found that PDMS copied and replicated surfaces have almost identical surface texture morphology to that of laser treated surface. Introducing synthesized silica particles improved the lotus effect on the PDMS copied and replicated surfaces; in which case, the hysteresis of droplet contact angle remains significantly low. © 2016 Wiley Periodicals, Inc. J. Appl. Polym. Sci. **2016**, *133*, 44015.

KEYWORDS: colloids; manufacturing; nanostructured polymers; optical properties

Received 27 March 2016; accepted 1 June 2016
DOI: 10.1002/app.44015

INTRODUCTION

Self-cleaning of surfaces in relation to photovoltaic applications (PV) is challenging in terms of cost-effective processing and maintaining required optical properties of PV panel surface after cleaning. Hydrophobicity of optical surfaces is one of the key concerns towards achieving self-cleaning surface characteristics. Surface hydrophobicity, mainly, depends on surface free energy and surface texture, similar to the surfaces that are widely observed in nature, such as lotus leaves, rice leaves, red rose petals, fish scales, etc.[1–5] Low surface free energy and micro/nano-textures create lotus effect, which is essential for self-cleaning applications. Some of the popular techniques towards achieving improved surface hydrophobicity include phase separation,[6] electrochemical deposition,[7] plasma treatment,[8] sol–gel processing,[9] electrospinning,[10] and solution immersion.[11] Micro/nano-texturing of surfaces have many challenges in terms of cost, processing time, and equipment. The precision of operation is the crucial factor to achieve desired surface textures composing of micro/nano pillars. Laser surface texturing provides the precision of operation, low cost, and short processing time; in which case, laser controlled ablation can be used effectively to texture surfaces at micro/nano levels.[12] Laser controlled ablation of optically transparent surfaces such as polycarbonate PV protective covers requires excessive efforts, which makes the process expensive.[12] In addition, extremely low thermal conductivity of the substrate material causes the formation of high thermal stresses due to excessive temperature gradients formed in laser irradiated region. On the other hand, texturing of ceramic surfaces, such as alumina (Al_2O_3), under laser-controlled ablation provides hydrophobic surface structures. Ceramics are, in general, opaque to solar radiation and could not be used as a protective cover of PV panels. However, replicating laser-textured surfaces by using polydimethylsiloxane (PDMS) can provide hydrophobic characteristics at the surface with high optical transmittance. In addition, PDMS replication of laser-textured surfaces can be repeated to obtain large area of hydrophobic surfaces with high optical transmittance, i.e., laser textured surface can be used as a mold to create optically transparent wafer with hydrophobic surface characteristics. Consequently, examination of laser texturing of a ceramic surface and replicating of the textured surface by PDMS becomes fruitful.

Considerable research studies were carried out to examine laser texturing of ceramic surfaces by a laser beam. Laser texturing of a ceramic surface with the presence of TiC and B_4C was studied by Yilbas.[13] He demonstrated that surface texture comprising of micro/nano poles and cavities was formed after laser ablation/melting process. Laser treated surface had a hydrophobic characteristic, which resulted in averaged contact angle of 130°.

Laser ablation of rare-earth oxide ceramics towards achieving superhydrophobic surfaces was carried out by Azimi *et al.*[14] They showed that laser textured surfaces had excellent water repellency due to improved surface hydrophobicity. Laser texturing of alumina surface for improved hydrophobicity was carried out by Yilbas *et al.*[15] Their findings revealed that Wenzel and Cassie and Baxter states were present at the treated surface due to the variation in the surface texture; overall, laser texturing improved the surface hydrophobicity. Tribology and superhydrophobicity of laser-controlled-melted alumina surfaces were investigated by Yilbas *et al.*[16] The findings revealed that laser treatment produced micropoles, nanopoles, and small size cavities at the surface, which enhanced the hydrophobicity of the surface. Replication of laser micromachined pattern in epoxy/alumina nanoparticle composite towards achieving superhydrophobic surfaces was carried out by Psarski *et al.*[17] They indicated that chemical hydrophobization with perfluorotetradecyltriethoxysilane (PFTDTES) provided superhydrophobic behavior in replicas with a water contact angle of 160° and a sliding angle of 8°. Superhydrophobic flaky γ-alumina coating on stainless steel surface was presented by Zhang *et al.*[18] They showed that the γ-alumina coating became much softer after transforming from flat to flaky form. In addition, the flaky γ-alumina coating exhibited a phenomenon of time-dependent plasticity and some flexibility. Laser-induced hydrophobicity of alumina surface was studied by Jagdheesh.[19] He showed that the geometry of the laser-machined pattern played a major role in changing the wetting properties rather than the chemical changes induced on the surface. Modification of sol–gel-derived amorphous alumina thin films via excimer laser irradiation was examined by Takeda *et al.*[20] It was reported that the elimination of CO caused the marked change in structure and surface properties of the film.

Polydimethylsiloxane (PDMS) is one of the candidates towards improving surface hydrophobic characteristics. Considerable research studies were carried out to investigate surface hydrophobic characteristics by using PDMS. Fabrication of PDMS micro/nano hybrid surface for increasing hydrophobicity was studied by Kim *et al.*[21] The micro/nano hybrid PDMS surface resulted in a higher water contact angle as compared with those of flat, nano-patterned, and micro-patterned PDMS surfaces. Hydrophobic characteristics of PDMS surfaces subjected to laser micro/nano patterning were investigated by Jeong *et al.*[22] They indicated that laser texturing resulted in superhydrophobic characteristics at the surface. Hydrophobicity of micro-structured PDMS surfaces was examined by Yeo *et al.*[23] They showed that the micro-pillars of an intrinsically hydrophobic material with a high aspect ratio enhanced the hydrophobicity of the surface by altering the surface topology. Effect of surface nanostructuring of PDMS on wetting properties and hydrophobic recovery was studied by Vlachopoulou *et al.*[24] They showed that intense surface topography led to a significant delay in hydrophobic recovery of the surface. *In vitro* blood compatibility of modified PDMS surfaces as superhydrophobic and superhydrophilic materials was investigated by Khorasani and Mirzadeh.[25] They indicated that chemical structures, such as negative-charge polar groups and wettability, were important factors in blood compatibility of these surfaces and the superhydrophilic and superhydrophobic modified PDMS surfaces had excellent blood compatibility as compared to that of the unmodified PDMS surface. Investigation of highly hydrophobic hierarchical nano/micro roughness of polymer surface created via stamping and laser micromachining was carried out by Cardoso *et al.*[26] They reported that laser texturing produced hierarchal surface morphology comprising of micro/nano-scale structures and exhibiting water contact angles in excess of 160°. Fabrication of rough polydimethylsiloxane (PDMS) surface containing micro-, submicro- and nano-composite structures using a facile one-step laser etching method was presented by Jin *et al.*[27] They indicated that the micro-, submicro-, and nano-structures formed at the surface significantly enhanced the surface roughness and led to the unusual self-cleaning property, which could be used in micro-fluidic channels with diminished resistance.

Replicating micro/nano-textured surfaces by PDMS does not always yield a lotus effect while increasing hysteresis of water contact angles at hydrophobic surfaces. This is due to the inability to copy and replicate nano-size fibers/whiskers-like features due to the odd orientation of these fine size textures at the surfaces. In order to improve hydrophobicity of PDMS copied and replicated surfaces, inclusion of nano-size colloidal particles at PDMS surfaces becomes unavoidable. Considerable research studies were carried out to examine colloidal particles on PDMS surfaces. Two-dimensional nano-patterning via PDMS relief structures of polymeric colloidal crystals was studied by Nam *et al.*[28] They presented two-dimensional colloidal crystals derived from poly(methyl)methacrylate-microspheres with a diameter of 380 nm and a negative surface charge formed on the hemispherical micro-wells by electrostatic force using positively charged poly(allylamine hydrochloride)-coated PDMS as a template to produce multidimensional nanostructures. Micro-patterns of colloidal assembly on chemically patterned surfaces were examined by Choi and Park.[29] The findings revealed that the aqueous suspension with ethanol offered improved results of the microarrays of colloidal assembly with ordered microstructures because of the low surface tension and fast evaporation rate of ethanol. Investigation of the assembly of micro-size glass spheres on structured surfaces via dewetting was carried out by Tull and Bartlett.[30] The assembly of spheres into the pits was found to be possible only when the pits were hydrophilic and the top surface hydrophobic. Hydrophobic surfaces of fibrous materials with core-shell latex particles were studied by Nguyen *et al.*[31] They developed a one-step method based on the filtration of the colloidal particles to obtain water-repellent fibrous materials such as paper or textiles that maintained stable properties even after several washing/drying cycles. Synthesis and colloidal stability of poly(*N*-isopropylacrylamide) microgels was investigated by Zha *et al.*[32] They demonstrated that particle sizes and swelling ratios depended on the reactions, which was due to the pH dependence of the degree ionization of the decomposed fragments originating from the initiators and their hydrophilicity–hydrophobicity characteristics.

Although laser texturing of alumina surfaces towards improving hydrophobic characteristics of the surface was studied earlier,[15,16] PDMS replicating of textured surfaces with the

Table I. Laser Treatment Conditions

Feed rate (m/s)	Power (W)	Frequency (Hz)	Nozzle gap (mm)	Nozzle diameter (mm)	Focus diameter (mm)	N_2 pressure (kPa)
0.1	2000	1500	1.5	1.5	0.3	600

inclusion of colloidal particles towards further reducing hysteresis angle and improved optical transmittance is left for the future study. In the present study, PDMS copying and replicating of laser-textured alumina surfaces is carried out. Improvement in surface hydrophobicity through deposition of synthesized nano-size silica particles on replicated and copied PDMS surfaces is investigated. Laser repetitive pulses are incorporated to create micro/nano size textures on alumina tile surfaces and high-pressure nitrogen assisting gas is used during the texturing process. One pot synthesis of silica particles is introduced to functionalize the surface of spherical silica particles in line with the previous study.[33]

EXPERIMENTAL

Alumina (Al_2O_3) tiles (Ceram Tec-ETEC, 2010) with 3 mm thickness were used as workpieces. The CO_2 laser (LC-ALPHAIII with wavelength 10.6 μm) was used to irradiate the alumina tile surfaces. The nominal output power of the laser was 2 kW and the irradiated spot diameter at the workpiece surface was about 200 μm. High pressure nitrogen gas jet emerging from the conical nozzle was utilized during the laser heating of the surfaces. The laser pulsing frequency was set at 1,500 Hz, which in turn gave rise to about 68% overlapping ratio for the irradiated spots at the surface. Laser treated surface properties were dependent on the proper selection of the laser

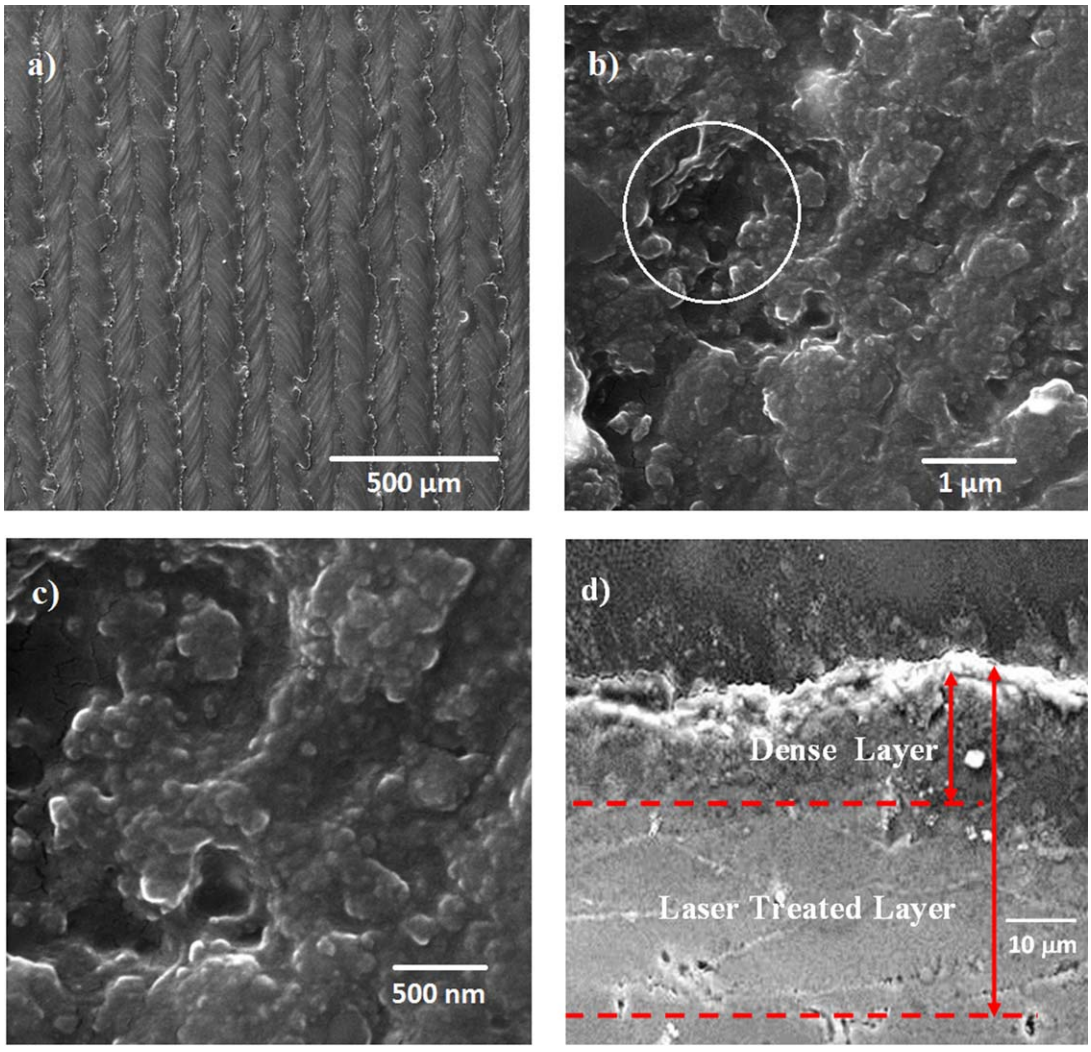

Figure 1. SEM micrograph of laser textured surfaces: (a) regular laser scanning tracks, (b) small cavity formed at the surface (marked in a white color circle), (c) fine size textures, and (d) cross section of laser treated region. [Color figure can be viewed in the online issue, which is available at wileyonlinelibrary.com.]

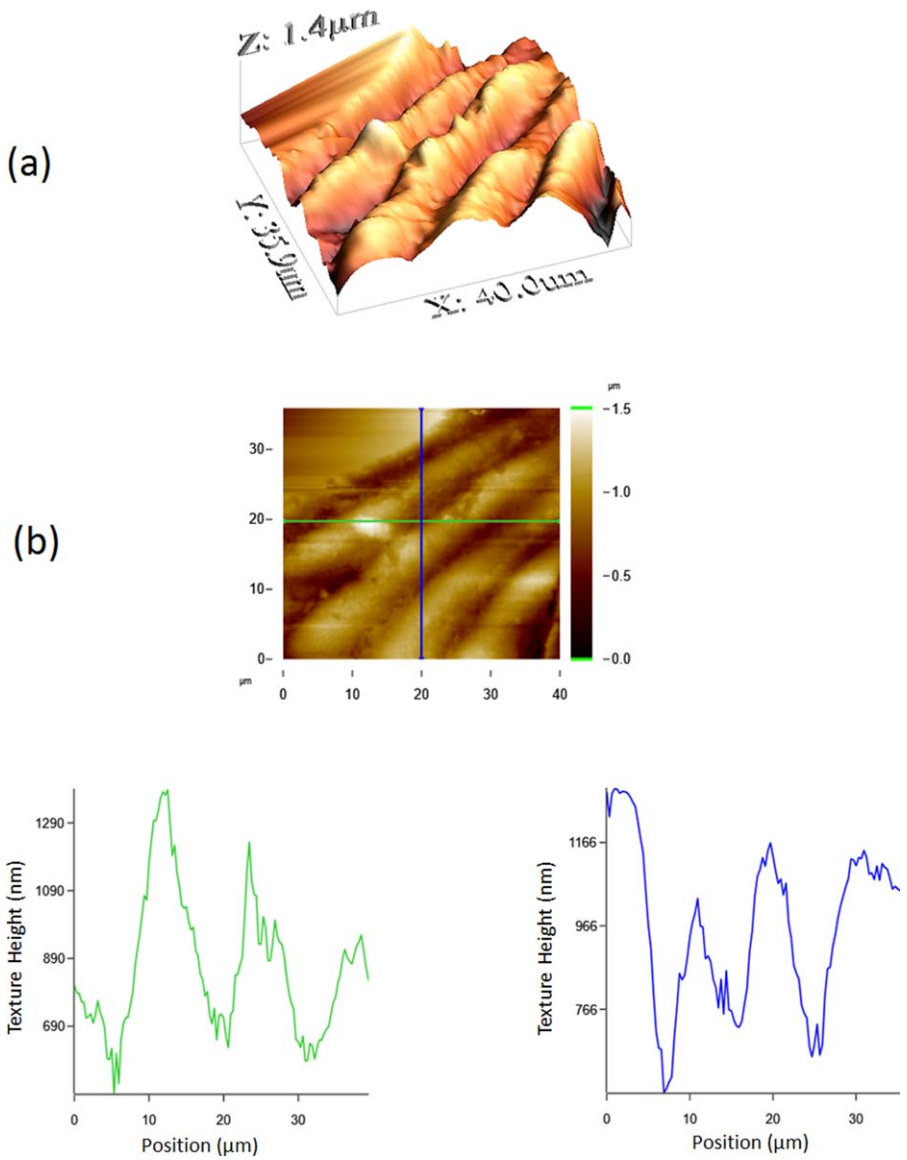

Figure 2. AFM images of laser treated surface: (a) three-dimensional view and (b) line scan showing texture heights at treated surface. [Color figure can be viewed in the online issue, which is available at wileyonlinelibrary.com.]

processing parameters. Therefore, through controlling the laser power settings, beam intensity distribution, pulse repetition rate, spot size, and the scanning speed, crack free surface texture could be realized. Laser treatment conditions are given in Table I.

Liquid polydimethylsiloxane (PDMS), which belongs to a group of polymeric organosilicon compounds, was used to replicate laser-textured surface. PDMS (Sylgard 184, Dow Corning) was prepared by mixing the elastomer base with hardening agent in 10:1 wt %. The mixture was deposited onto the laser textured surface and degasified in a vacuum chamber at 0.1 bar for 30 min. The deposited and degasified PDMS was left in the oven at 150°C for 30 min for curing purposes. Solidified PDMS was then removed from laser textured surface after the curing period was over. PDMS was prepared again in 10:1 wt % (elastomer base to hardening agent ratio), poured over the copied PDMS, degassed, and then cured in an oven using same parameters.

The procedure adopted for synthesizing of silica nano particles was similar to that reported in the previous study.[33] The process is briskly described herein. Tetraethyl orthosilicate (TEOS) and isobutyltrimethoxysilane (OTES), ethanol, and ammonium hydroxide were used in the synthesizing process. In this case, 14.4 mL of ethanol, 1 mL of ultrapure water, and 25 mL of ammonium hydroxide were mixed and stirred for 12 min. Later, 1 mL of TEOS was diluted with 4 mL of ethanol and added to the mixture. Following 30 min after this process, 0.5 mL of TEOS diluted in 4 mL ethanol was added. After 5 min, a modifier silane molecule was added in a molar ratio of 3:4 with respect to the second edition of TEOS. The final mixture was stirred for 20 h at room temperature, and later centrifuged and washed with ethanol for removal of reactants. The solvent

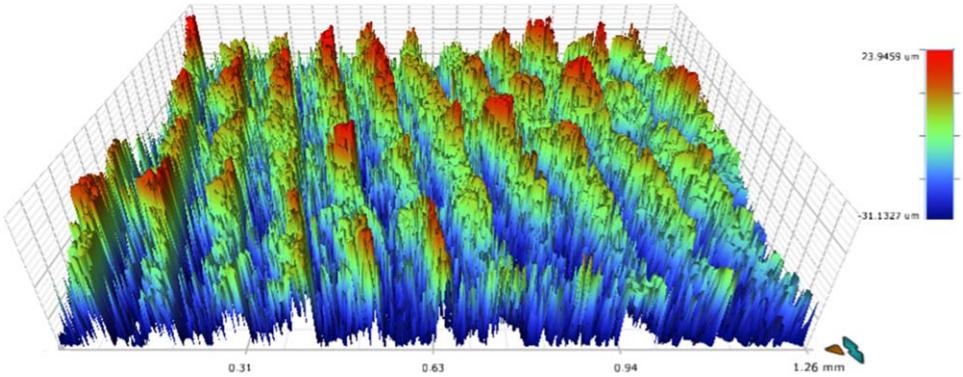

Figure 3. Three-dimensional optical image of the laser textured surface. [Color figure can be viewed in the online issue, which is available at wileyonlinelibrary.com.]

casting was applied to deposit the solution onto PDMS copied and replicated surfaces. Upon vacuum drying, until all solvent was evaporated, characterization of resulting surfaces was carried out.

Material and surface characterization of laser textured, PDMS copied and replicated, and synthesized silica particles deposited surfaces was carried out using scanning electron microscope (SEM) Jeol 6460. X-ray diffraction (XRD) measurements were performed on Bruker D8 Advanced having CuKα radiation. A typical setting of XRD was 40 kV and 30 mA and scanning angle (2θ) was ranged 20°–80°. Atomic Force Microscopy/Scanning Probe Microscopy (AFM/SPM) Microscope in contact mode was used to analyze the surface texture. The tip was made of silicon nitride (r = 20 – 60 nm) with a manufacturer specified force constant, k, of 0.12 N/m. X-ray photoelectron spectroscopy (XPS) measurements were performed in an ESCALAB 200-X spectrometer (VG Instrument) using non-monochromatized AlK_{α} radiation (1,486.6 eV) from a twin Mg/Al anode operating at 300 W. The system was equipped with 4 KV differential pumped argon-ion gun for depth profile study of workpieces. Ar^{+} ions with energy 2 keV were used for this purpose. The ion current was maintained at 3 μm/cm^2. The material removal rate was estimated as 0.3 nm/min.

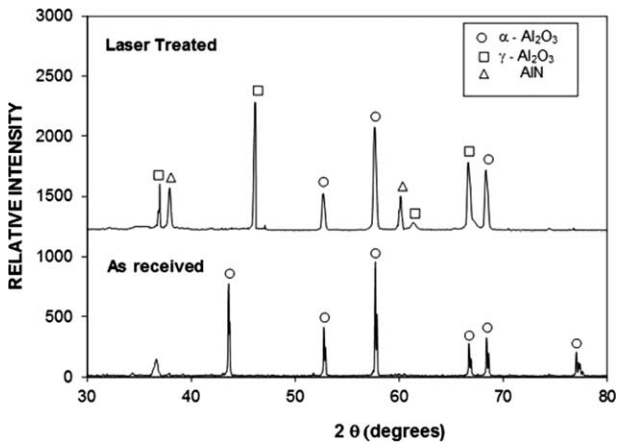

Figure 4. X-ray diffractogram of as received and laser treated alumina surface.

Fourier transform infrared spectroscopy (FTIR) was carried out incorporating Nicolet Nexus 670 FTIR Spectrometer. The wetting experiment was performed using Kyowa (model - DM 501) contact angle goniometer. A sessile drop method was considered for the contact angle measurements. The water contact angle between the water droplet and the surface was measured with the fluid medium as de-ionized water. Droplet volume was controlled with an automatic dispensing system having a volume step resolution of 0.1 μL. Still images were captured, and contact angle measurements were performed after 1 sec of deposition of water droplet on the surface. UV–VIS Spectrophotometer (Jenway 67 series) was used to measure the transmittance of PDMS copied and replicated workpieces prior and after synthesized colloidal particles deposition.

RESULTS AND DISCUSSION

Laser texturing of alumina surface is carried out under high-pressure nitrogen assisting gas. Laser textured surfaces are copied and replicated by using Polydimethylsiloxane (PDMS). To create the lotus effect and increase the surface hydrophobicity of PDMS copied and replicated surface, synthesized silica particles are introduced at the surface. The resulting surface characteristics are analyzed using the analytical tools.

Figure 1 shows SEM micrograph of a laser textured alumina surface while Figure 2 shows AFM images of three-dimensional textured surface [Figure 2(a)] and texture profile along the surface line scan [Figure 2(b)]. In addition, three-dimensional optical image of the laser-textured surface is shown in Figure 3. Laser treated surface consists of regular laser scanning tracks [Figure 1(a)], which are formed by the irradiated spots at the surface during the laser repetitive pulse heating. Since the laser pulsing frequency is 1,500 Hz, the overlapping ratio of the consecutive irradiated spots is in the order of 70%. Although laser controlled melting and ablation at the surface results in high temperature gradients in the surface region,[34] no thermally induced crack is observed at the surface. The crack free laser treated layer is also seen from SEM micrograph of the cross section of the laser treated section [Figure 1(d)]. In this case, a dense layer is formed at the surface because of the high cooling rates. The crack free layer is associated with the closely spaced

Table II. EDS Data (wt %) of Laser Treated Alumina Surface

Spectrum	N	O	Al
Spectrum 1	4.3	41.2	Balance
Spectrum 2	4.8	40.8	Balance
Spectrum 3	4.4	41.2	Balance

laser scanning tracks at the surface. In this case, heat conduction from recently formed laser scanning tracks towards the previously formed tracks modifies the cooling rate below the surface. This, in turn, creates a self-annealing effect in the treated region while lowering the thermal stresses formed in the treated layer. Moreover, laser power intensity across the irradiated spot is Gaussian, which gives rise to the occurrence of the laser peak intensity at the irradiated spot center. This results in surface evaporation at the irradiated spot center and melting towards the irradiated spot edges. Therefore, a small cavity forms at the irradiated spot center [Figure 1(b)]. However, the melt flow from the neighboring irradiated spot modifies the cavity size during the consecutive pulses. This causes the formation of textures with micro/nano size features at the surface [Figure 1(c)]. This situation is also observed from Figures 2(a) and 3, in which three-dimensional image of the surface is shown. Since the regular laser scanning tracks take place at the surface, the hierarchical texture consisting of micro/nano poles is formed on the laser treated surface. The texture height varies, which can be seen from Figure 2(b) and the average surface roughness is in the order of 0.82 μm. Figure 4 shows X-ray diffractogram of laser treated and as received surfaces. Since nitrogen at high pressure is used as an assisting gas during laser texturing of alumina surfaces, the nitride compound (AlN) is formed at the surface, which is visible from the X-ray diffractogram of the surface. The peaks appeared in the X-ray diffractogram include Al_2O_3 (ICSD Collection Codes 010426 & 073076), AlN (ICSD Collection Codes 041358 & 082790), and AlN (ICSD Collection Codes 070032 & 070033). The aluminum nitride is formed according to the following reactions. In the first step, a single alumina oxide and carbon monoxide are formed at the treated surface through a reaction $Al_2O_3 + 2C \rightarrow Al_2O + 2CO$. In the following step, AlN compound is formed through the reaction $Al_2O + CO + N_2 \rightarrow 2AlN + CO_2$ under the high pressure nitrogen environment during laser treatment process.[35] Energy dispersive spectroscopy (EDS) is carried out to assess the elemental changes at the surface after the laser texturing. The elemental composition of the laser-textured surface is given in Table II. The data reveals that the elemental composition does not alter notably at the laser treated surface. However, nitrogen presence in EDS data indicates the formation of nitride species at the surface, despite the fact that the precise quantification of nitrogen is difficult in the EDS system because of being a light element. To confirm the presence of AlN at the laser treated surface, XPS measurements were carried out. The XPS spectral lines for AlN, as shown in Figure 5, reveals the presence of Al and N peaks. The Al 2p line is centered at 74.3 eV [Figure 5(a)] and N 1s line at 399 eV [Figure 5(b)]. These lines are in similar position to those shown in the literature.[36] Consequently, AlN compound is formed during the laser processing of the surface.

Figure 6 shows SEM micrographs of PDMS replicated surfaces. PDMS replicated and laser textured surface are almost identical in terms of surface morphology [Figures 1(a) and 6(a)]; in which case, the presence of laser scanning tracks are evident on the PDMS copied and replicated surfaces. However, close examination of the replicated surfaces reveals that some of the texture details are not replicated properly [Figure 6(b,c)]. In this case, some nano-size whiskers-like texture are not copied onto

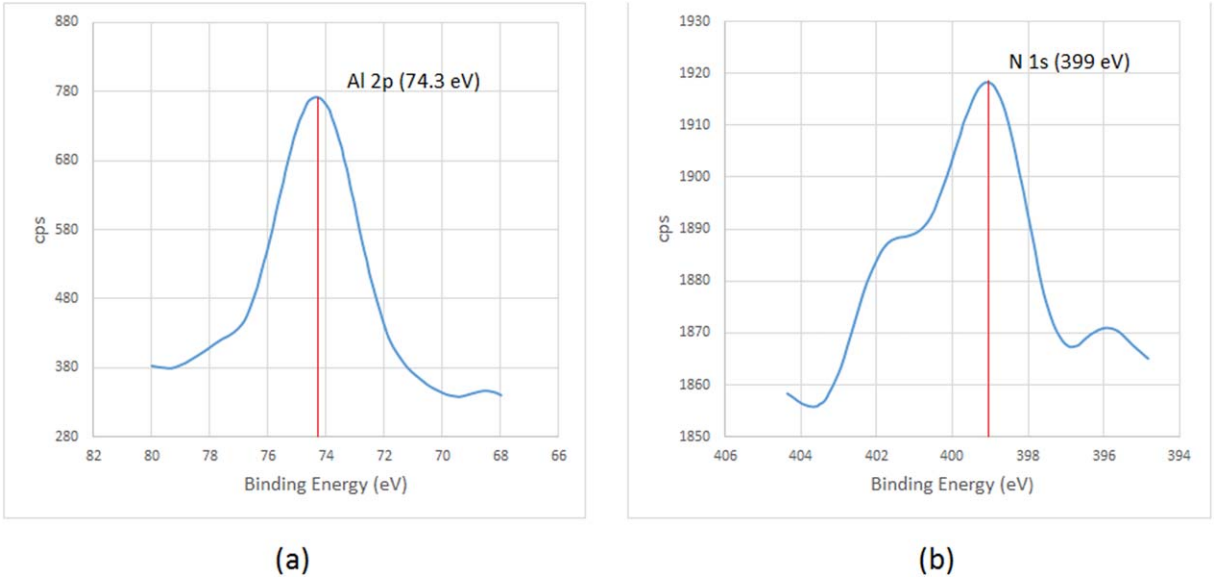

Figure 5. XPS Spectral Lines for AlN: (a) Aluminum 2p line and (b) Nitrogen 1s line. [Color figure can be viewed in the online issue, which is available at wileyonlinelibrary.com.]

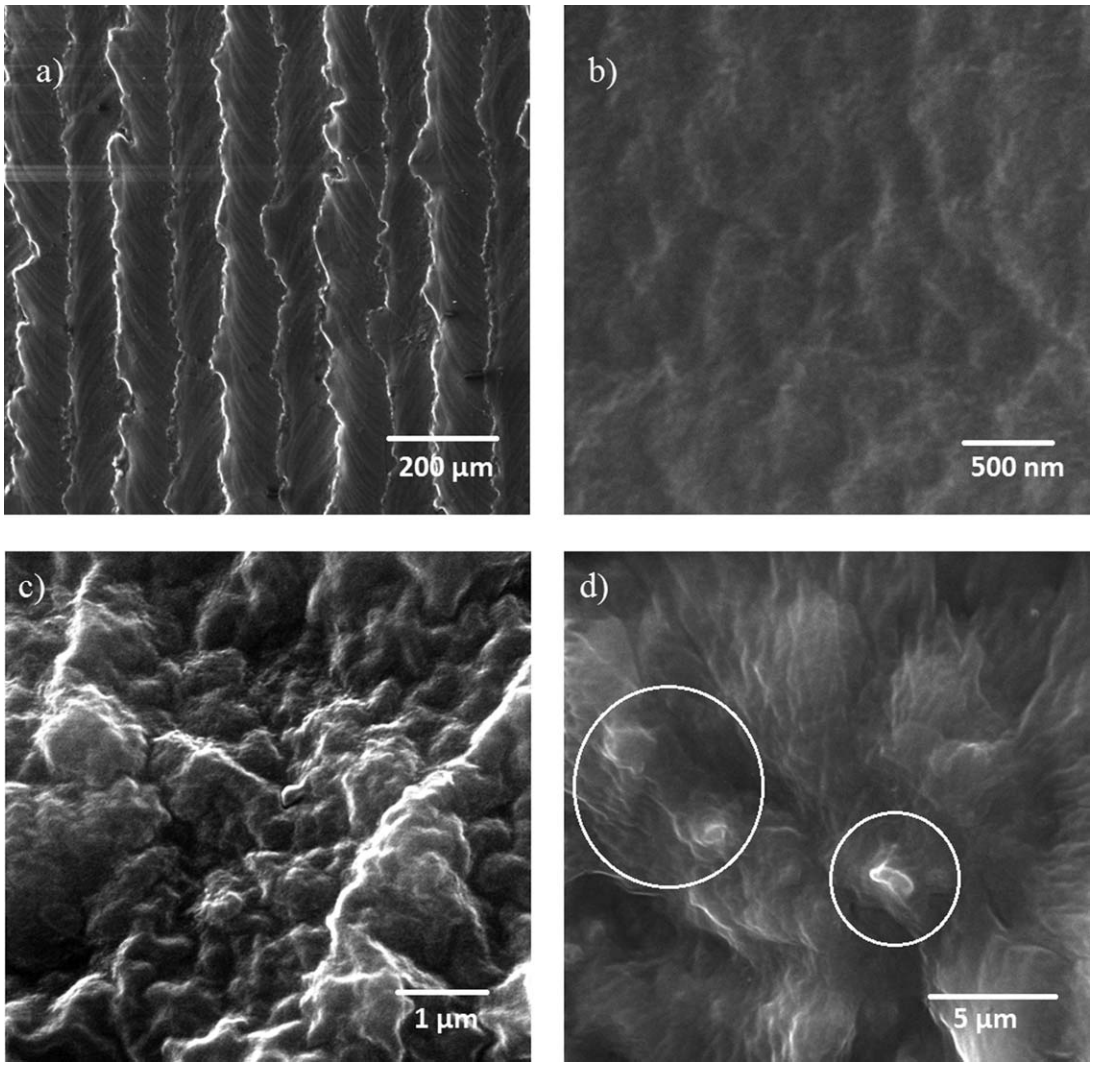

Figure 6. SEM micrographs of PDMS replicated of laser-textured surfaces: (a) regular laser scanning tracks, (b) textured surface, (c) fine size textured morphology, and (d) some AlN residues on the surface.

PDMS surface. This is associated with the irregular alignment of these whiskers-like textures on the laser treated surface; therefore, during peeling of PDMS from the laser-textured surfaces, these textures are broken and remained as residues in the PDMS copied surface. This situation is also seen from Figure 6(d), in which the presence of alumina residue on the PDMS replicated surface is evident. Figure 7 shows AFM images of PDMS copied and replicated surfaces. Three-dimensional image [Figure 7(a)] shows that PDMS copied surface composes of micro/nano textures with hierarchical structures. This is also true for PDMS replicated surface [Figure 7(b)]. However, line scan at PDMS copied surface shows that some of the nano-size sharp waviness, as observed for the laser textured surface [Figure 2(b)], is replaced with rounded waviness. The same observation is made for the PDMS replicated surface. This is due to the broken pieces of nano-size whiskers-like structures during the removal of PDMS from the laser treated surface. In this case, the broken parts remain as residues on the PDMS copied and replicated surfaces. The average surface roughness of the PDMS copied and replicated surface are in the order of 0.72 µm and 0.87 µm, respectively. The small deviation of the average surface roughness is associated with the geometric feature of the surface texture. In this case, valleys on PDMS copied surface become hills on PDMS replicated surface since PDMS copied surface is used as a mold for replicated PDMS surface.

Since nano-size whiskers could not be copied and replicated, synthesized nano-size silica particles are introduced at PDMS copied and replicated surfaces to generate lotus effect. It should be noted that nano-size texture is crucial to create a lotus effect on the surfaces, which lowers the contact angle hysteresis on the treated surface. Figure 8 shows SEM micrographs of functionalized silica particles deposited onto PDMS replicated surfaces. The deposited silica particles cover extensively PDMS replicated surfaces and they are closely spaced on the surface [Figure 8(b)]. Since tetraethyl orthosilicate (TEOS) is used during the synthesizing of silica particles, the functionalized shell distorts

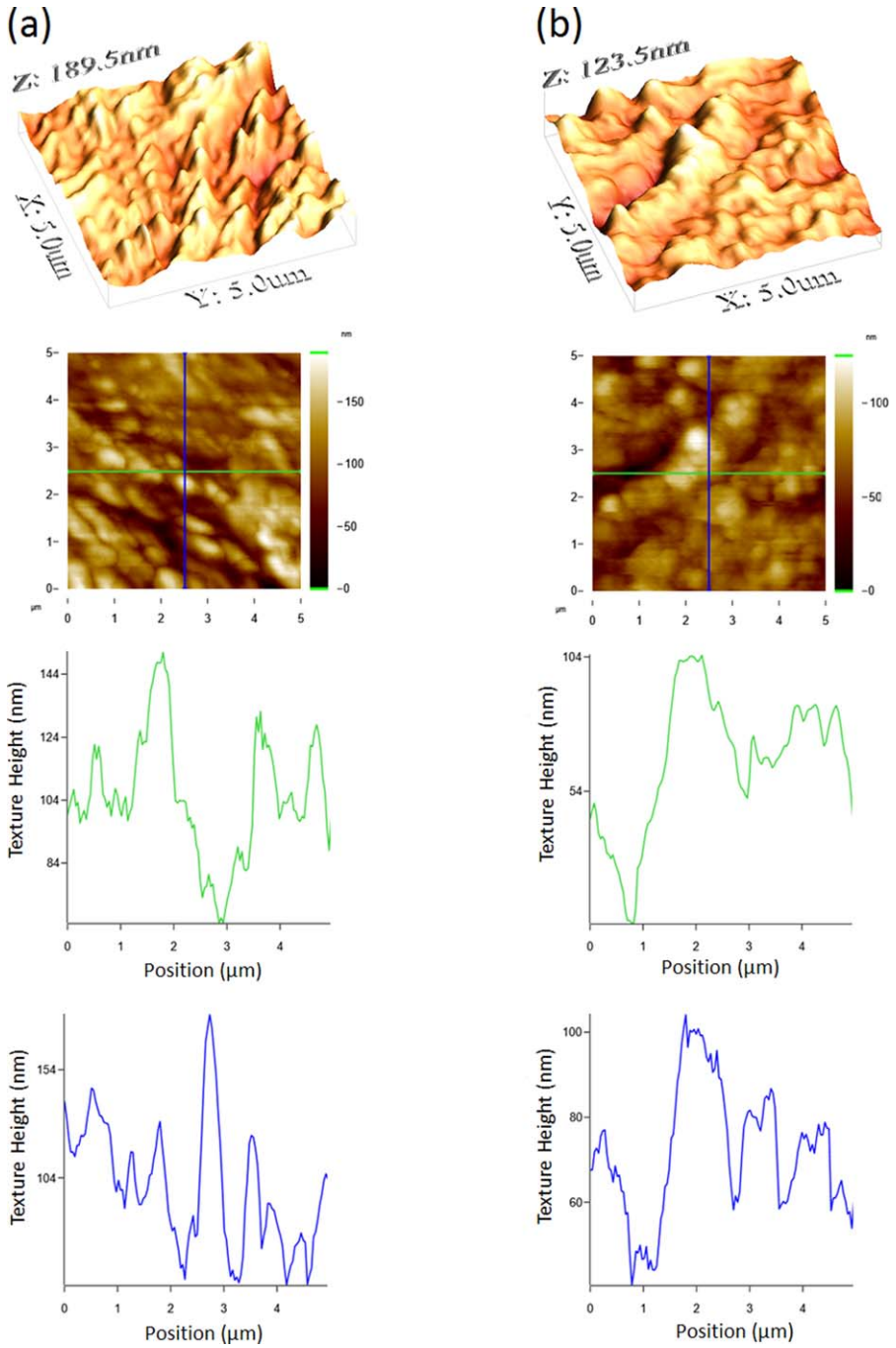

Figure 7. AFM images of PDMS copied and replicated surfaces, and line scan showing the texture heights at the surface: (a) PDMS copied surface and (b) PDMS replicated surface. [Color figure can be viewed in the online issue, which is available at wileyonlinelibrary.com.]

the surface roughness of the particles; in which case, a small increase in the cell size occurs.[37] This can be related to the condensing monomer units, which are growing at a faster rate than the nucleation rate.[33] Since diluted TEOS concentration with ethanol is incorporated during synthesizing of silica particles, the rate of formation of new nuclei is suppressed. This, in turn, resulted in aggregation and adhesion of the particles [Figure 8(c,d)]. It should be noted that the hydroxyl groups on the functionalized silica particle surfaces have different moieties and can have different reactivity towards the modifier molecules. Hence, modifier silane results in side reactions and condensation on the silica surface.38 Figure 9 shows AFM images of PDMS replicated surface after deposition of functionalized silica particles. The surface texture does not change considerably after the deposition of silica particles on PDMS replicated surfaces, which can be observed from the three-dimensional image of the surface [Figure 9(a)]. The presence of silica particles is evident from the line scan [Figure 9(b)]. Since no loose silica particles are observed from SEM micrographs (Figure 8) and AFM images (Figure 9), functionalizing silica particles prior to

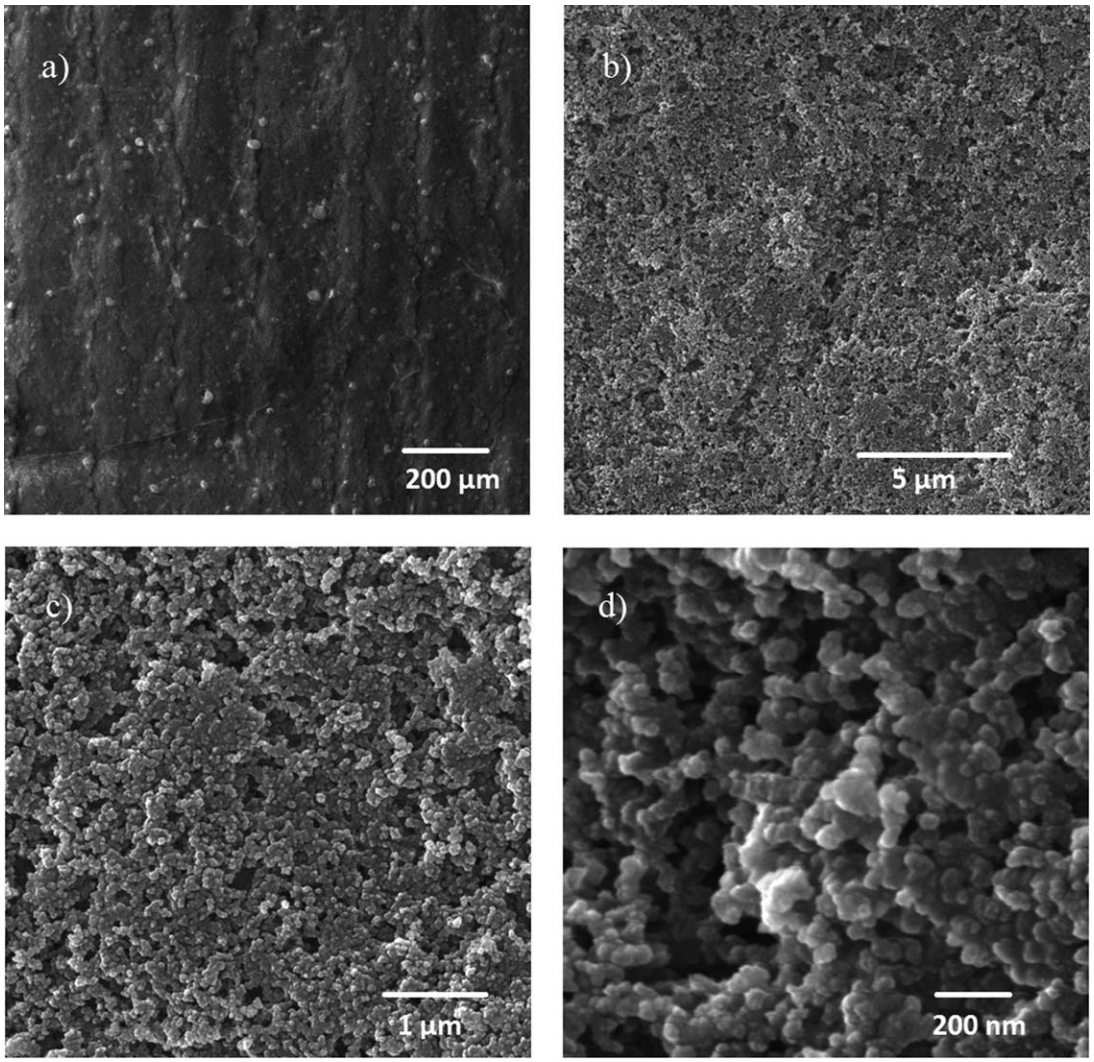

Figure 8. SEM micrographs of PDMS replicated and functionalized silica particles deposited surface: (a) functionalized particles on replicated surface, (b) large coverage area at PDMS copied surface, (c) aggregated functionalized silica particles, and (d) spherical shape of functionalized and aggregated particles.

deposition onto PDMS replicated surface improves the adhesion between the particles and the surface.

Figure 10 shows FTIR data for PDMS copied and replicated surfaces. PDMS sample without copying and replicating is also included for the comparison reason. In general, two groups of data are visible from FTIR spectrums, namely Si–Methyl (SiMe) and siloxane (SiOSi) groups. A doublet at 1,100 cm^{-1} and 1,020 cm^{-1} correspond to asymmetric and symmetric stretching vibration, respectively.[39] The SiMe structure peak occurs at 1,250 cm^{-1}.[40] Slight differences in absorption as compared to that reported in the literature[41] are associated with the solidification rates of liquid PDMS, which takes longer duration for solidification at laser-textured surface while slightly modifying the absorption characteristics. The presence of absorption peak at 2,960 cm^{-1} corresponds to $–CH_3$ (asymmetric) bend stretching vibration.[42] In addition, the presence of a peak at 670 cm^{-1} is due to the Al–N vibrations taking place for the PDMS copied and replicated samples. This is attributed to the residues of textured alumina surfaces, such as whiskers, which remain in the PDMS copied surface after removal from laser-textured surface. In the case of FTIR, data for PDMS copied and replicated samples after the deposition of functionalized silica particles, the regular PDMS peaks are observed as similar to PDMS copied and replicated samples. The peak at 800 cm^{-1} is related to the bending modes of Si–O–Si. In addition, the occurrence of a peak at 3,420 cm^{-1} is related to stretching vibrations O–H on the silica surface, which indicates that the surfaces are not fully covered with the grafted groups. The absorption peak at 1,400 cm^{-1} is attributed to the bending modes of C–H of any organic residues.43 Figure 11 shows UV transmittance data for PDMS copied and replicated as well as silica nano particles deposited samples. The data for as received PDMS sample are also included for the comparison reason. UV transmittance of PDMS copied and replicated samples reduce slightly compared to that of the as-received flat PDMS sample.

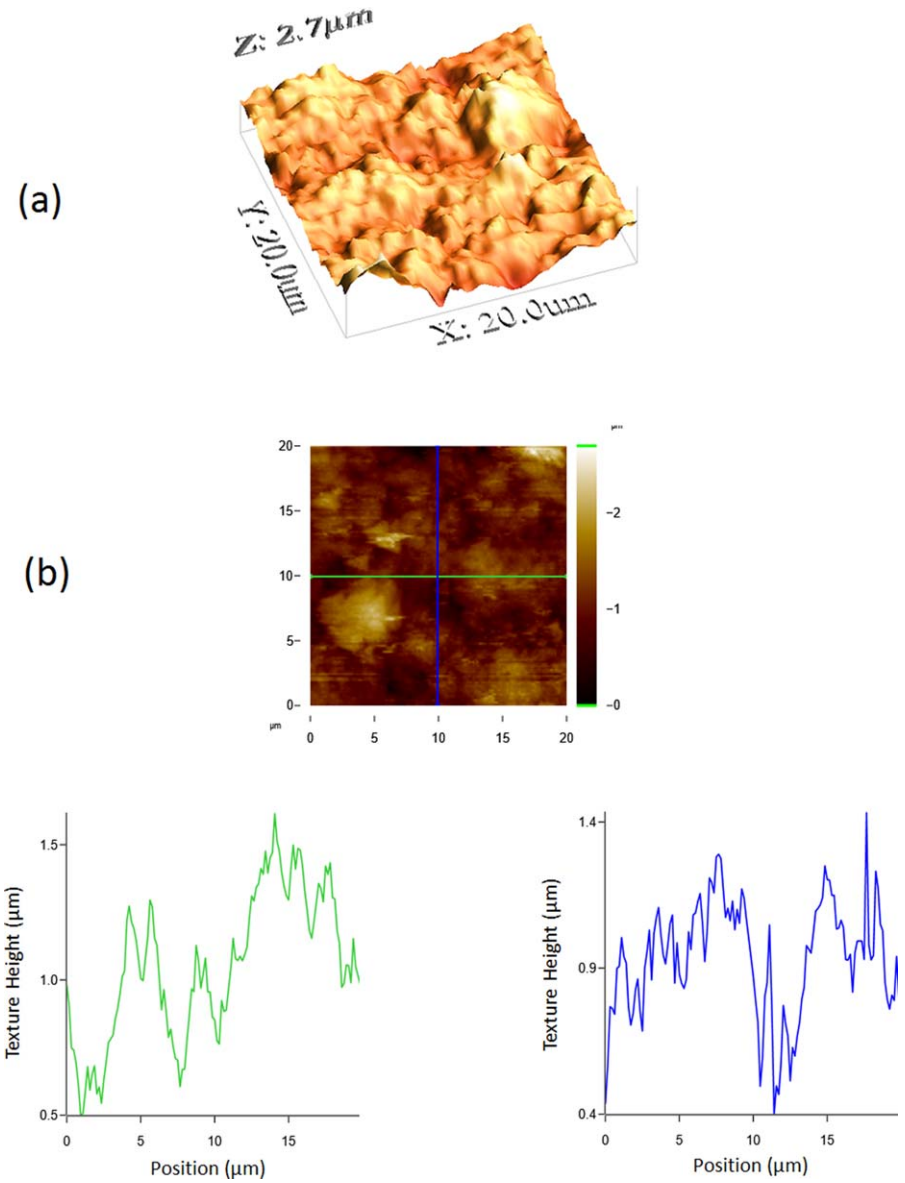

Figure 9. AFM image of PDMS replicated and functionalized silica particles deposited surface: (a) three-dimensional surface texture, and (b) line scan showing the texture height at the surface. [Color figure can be viewed in the online issue, which is available at wileyonlinelibrary.com.]

Deposition of silica particles on PDMS copied and replicated surfaces further lowers the UV transmittance for the wavelength range 300 nm to 550 nm. However, as the wavelength increases, transmittance improves for functionalized silica particle deposited PDMS copied and replicated surfaces.

Figure 12 shows images of water droplets on laser textured, PDMS copied, PDMS replicated, and colloidal particles deposited surfaces. Water droplet contact angle remains high for the laser-textured surface, and then follows colloidal particles deposited surfaces, PDMS replicated, and PDMS copied surfaces. In this case, low surface energy, due to AlN compounds formed at the surface, and texture of laser treated alumina surface resulted in high water droplet contact angle. The contact angle of the droplets varies within 10% over the laser treated surface. This is associated with one or all of the followings: (1) surface free energy of laser treated sample (51.6 ± 4 mJ/m^2) varies across the surface because of non-uniform distribution of AlN compounds at the surface, and (2) non-homogeneous texture morphology of laser-treated surface. Nevertheless, the area covered for high contact angle is considerably larger than that of low contact angle region; in which case, the high contact angle region is in the order of 93% of the total area of the laser treated surface. Since whiskers-like geometric features could not be copied by PDMS, the lotus effect is suppressed. This, in turn, gives rise to the attainment of relatively lower water droplet contact angle for PDMS copied and replicated surfaces than that of laser treated surface. This situation can be seen from Table III, in which droplet contact angle and hysteresis are given. It should be noted that contact angle hysteresis is determined from $\theta_{hysteresis} = \theta_{Advancing} - \theta_{Receding}$, where $\theta_{Advancing}$ is

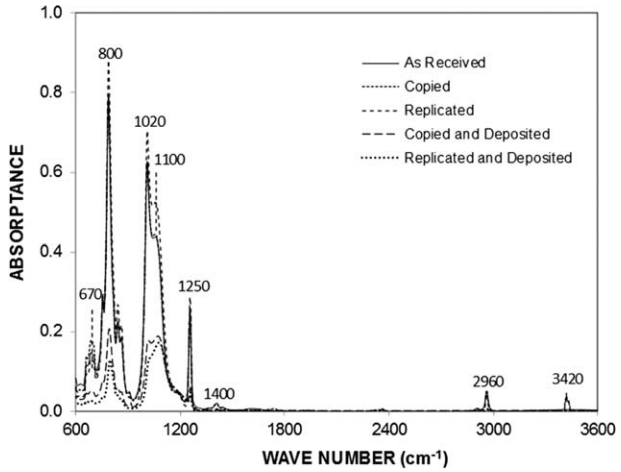

Figure 10. FTIR data for as received, and PDMS copied and replicated as well as functionalized silica particles deposited surfaces.

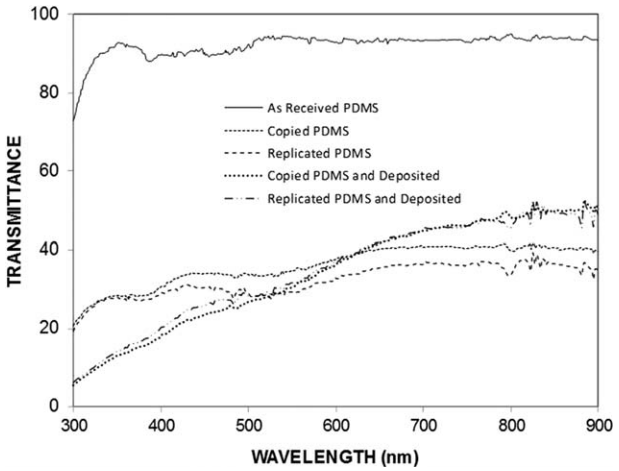

Figure 11. UV transmittance of as received and PDMS copied and replicated as well as functionalized silica particles deposited samples.

the advancing angle and $\theta_{Receding}$ is the receding angle. Deposition of functionalized silica particles on PDMS copied and replicated surfaces increases water droplet contact angle and reduces significantly contact angle hysteresis. Consequently, nano-size silica particles create lotus effect on the deposited surfaces.

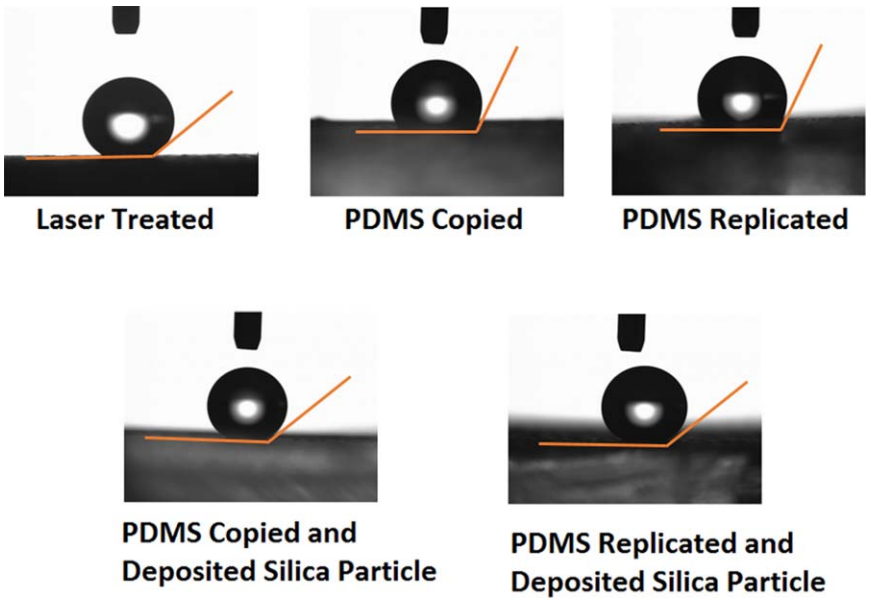

Figure 12. Images of water droplets used for contact angle measurements. [Color figure can be viewed in the online issue, which is available at wileyonlinelibrary.com.]

Table III. Contact Angle Data and Hysteresis for as Received and Laser Treated Surfaces, PDMS Copied/Replicated Surfaces, and PDMS Copied/Replicated and Functionalized Silica Particles Deposited Surfaces

	Contact angle (degrees)	Hysteresis (degrees)
Untreated surface	65.3 (+5/−5)	42 (+3/−3)
Laser-treated surface	150.3 (+5/−5)	18 (+5/−5)
PDMS copied	122.62 (+0.2/−0.2)	17 (+1.8/−1.8)
PDMS replicated	123.7 (+1.1/−1.1)	20.9 (+1.9/−1.9)
PDMS copied and deposited	157 (+1.5/−1.5)	4.0 (+3.3/−3.3)
PDMS replicated and deposited	155.5 (+0.8/−0.8)	2.6 (+1.9/−1.9)

CONCLUSIONS

Laser texturing of alumina surfaces is carried out under high-pressure nitrogen environments towards achieving hydrophobic surfaces. Since the textured surfaces are optically opaque, polydimethylsiloxane (PDMS) is introduced to copy and replicate laser-textured surfaces. Functionalized silica particles are deposited at the surface to lower the contact angle hysteresis and thus create a lotus effect. Tetraethyl orthosilicate (TEOS) mixed with ethanol solution is used to synthesized silica particles. Functionalization of silica particles gives rise to aggregation and improved adhesion onto PDMS surface. Surface morphology of laser textured, PDMS copied and replicated, and functionalized silica particles deposited samples are assessed using scanning electron and atomic force microscopes. To characterize the sample surfaces, X-ray diffraction, X-ray photoelectron spectroscopy, and Fourier-transform infrared spectroscopy are carried out. UV transmittance of PDMS copied and replicated as well as functionalized colloidal particles deposited samples is measured. Surface hydrophobicity of the samples is analyzed incorporating water contact angle measurements. It is found that laser controlled melting and evaporation of alumina surfaces results in surface texture composing of micro/nano features. Formation of AlN at the textured surface lowers the surface energy. Hence, micro/nano surface texture with low surface energy gives rise to high water droplet contact angles with low hysteresis. PDMS copied and replicated surfaces show similar surface morphology to that of the laser textured surfaces. However, whiskers-like nano-size structures at the laser-textured surface are not copied by PDMS because of their complex geometry. Consequently, water droplet contact angle reduces for PDMS copied and replicated surfaces. Deposition of functionalized silica particles gives rise to a significant improvement in water droplet contact angle. In this case, water droplet contact angle increases and hysteresis reduces considerably. UV transmittance data reveals that PDMS copying and replicating of laser textured surface results in a reduction in the transmittance. Further small reductions in transmittance are observed after functionalized silica particles are deposited onto PDMS copied and replicated surfaces.

ACKNOWLEDGMENTS

The authors acknowledge the financial support of King Fahd University of Petroleum and Minerals (KFUPM) through Project# MIT11111-11112 to accomplish this work.

REFERENCES

1. Wagner, T.; Neinhuis, C.; Barthlott, W. *Acta Zool.-Stockholm* **1996**, *77*, 213.
2. Parker, A. R.; Lawrence, C. R. *Nature* **2001**, *414*, 33.
3. Gao, X.; Jiang, L. *Nature* **2004**, *432*, 36.
4. Byun, D.; Hong, J.; Saputra Ko, J. H.; Lee, Y. J.; Park, H. C.; Byun, B. K.; Lukes, J. R. *J. Bionic Eng.* **2009**, *6*, 63.
5. Koch, K.; Bhushan, B.; Barthlott, W. *Soft Matter* **2008**, *4*, 1943.
6. Han, J. T.; Xu, X. R.; Cho, K. W. *Langmuir* **2005**, *21*, 6662.
7. Shirtcliffe, N. J.; McHale, G.; Newton, M. I.; Chabrol, G.; Perry, C. C. *Adv. Mater.* **2004**, *16*, 1929.
8. Kinoshita, H.; Ogasahara, A.; Fukuda, Y.; Ohmae, N. *Carbon* **2010**, *48*, 4403.
9. Latthe, S. S.; Imai, H.; Ganesan, V.; Rao, A. V. *Appl. Surf. Sci.* **2009**, *256*, 217.
10. Ma, M.; Mao, Y.; Gupta, M.; Gleason, K. K.; Rutledge, G. C. *Macromolecules* **2005**, *38*, 9742.
11. Cheng, Z.; Du, M.; Lai, H.; Zhang, N.; Sun, K. *Nanoscale* **2013**, *5*, 2776.
12. Yilbas, B. S.; Matthews, A.; Karatas, C.; Leyland, A.; Khaled, M.; Abu-Dheir, N.; Al-Aqeeli, N.; Nie, X. *J. Manuf. Sci. Eng.* **2014**, *136*, 054501.
13. Yilbas, B. S. *Ceram. Int.* **2014**, *40*, 16159. Ceram. Int.
14. Azimi, G.; Kwon, H.-M.; Varanasi, K. K. *MRS Commun.* **2014**, *7*, 95.
15. Yilbas, B. S.; Khaled, M.; Abu-Dheir, N.; Aqeeli, N.; Furquan, S. Z. *Appl. Surf. Sci.* **2013**, *286*, 161.
16. Yilbas, B. S.; Bhushan, H.; Aleem, B. J. A.; Gaseem, Z. *JOM-J. Min. Met. Mat. S.* **2014**, *66*, 1068.
17. Psarski, M.; Marczak, J.; Grobelny, J.; Celichowski, G. *J. Nanomater.* **2014**, *2014*, 547895.
18. Zhang, X.; Liu, X.; Laakso, J.; Levanen, E.; Mantyla, T. *Appl. Surf. Sci.* **2012**, *258*, 3102.
19. Jagdheesh, R. *Langmuir* **2014**, *30*, 12067.
20. Takeda, S.; Ikuta, Y.; Hirano, M.; Hosono, H. *J. Mater. Res.* **2001**, *16*, 1003.
21. Kim, D. S.; Lee, B.-K.; Yeo, J.; Choi, M. J.; Yang, W.; Kwon, T. H. *Microelectron. Eng.* **2009**, *86*, 1375.
22. Jeong, H.-M.; Lee, W.-Y.; Lee, J.-H.; Yang, D.-C.; Lim, K.-S. *Proc. SPIE Int. Soc. Optical Eng.* **2013**, *8612*, 2004368.
23. Yeo, J.; Kim, D. S. *Microsys. Technol.* **2010**, *16*, 1457.
24. Vlachopoulou, M.-E.; Petrou, P. S.; Kakabakos, S. E.; Tserepi, A.; Beltsios, K.; Gogolides, E. *Microelectron. Eng.* **2009**, *86*, 1321.
25. Khorasani, M. T.; Mirzadeh, H. *J. Appl. Polym. Sci.* **2004**, *91*, 2042.
26. Cardoso, M. R.; Martins, R. J.; Dev, A.; Voss, T.; Mendonca, C. R. *J. Appl. Polym. Sci.* **2015**, *132*, 42082.
27. Jin, M.; Feng, X.; Xi, J.; Zhai, J.; Cho, K.; Feng, L.; Jiang, L. *Macromol. Rapid Commun.* **2005**, *26*, 1805.
28. Nam, H. J.; Kim, J.-H.; Jung, D.-Y.; Park, J. B.; Lee, H. S. *Appl. Surf. Sci.* **2008**, *254*, 5134.
29. Choi, W. M.; Park, O. O. *Colloids Surf. A* **2006**, *277*, 131.
30. Tull, E. J.; Bartlett, P. N. *Colloids Surf. A* **2008**, *327*, 71.
31. Nguyen, D.; Chambon, P.; Rosselgong, J.; Cloutet, E.; Cramail, H.; Ravaine, S. *J. Appl. Polym. Sci.* **2008**, *108*, 2772.
32. Zha, L.; Li, L.; Bao, L. *J. Appl. Polym. Sci.* **2007**, *103*, 3893.
33. Yong, W. Y. D.; Zhang, Z.; Cristobal, G.; Chin, W. S. *Colloids Surf. A* **2014**, *460*, 151.
34. Yilbas, B. S.; Akhtar, S. S.; Karatas, C. *Surf. Eng.* **2011**, *27*, 470.
35. Huang, Z.; Cho, S.; Jiang, D.; Tan, S. *J. Mater. Sci.* **1999**, *34*, 2023.
36. Ji, A. L.; Ma, L. B.; Liu, C.; Li, C. R.; Cao, Z. X. *Diam. Relat. Mater.* **2005**, *14*, 1348.

37. van Blaaderen, A.; Kentgens, A. P. M. *J. Non-Cryst. Solids* **1992**, *149*, 161.
38. Lin, J.; Chen, H.; Ji, Y.; Zhang, Y. *Colloids Surf. A* **2012**, *411*, 111.
39. Aguiar, K. R.; Santos, V. G.; Eberlin, M. N.; Rischka, K.; Noeske, M.; Tremiliosi-Filho, G.; Rodrigues-Filho, U. P. *RSC Adv.* **2014**, *4*, 24334.
40. Smith, A. L. The Analytical Chemistry of Silicones; Wiley: New York, **1991**; Vol. *160*, pp. 320–329.
41. Gaboury, S. R.; Urban, M. W. *Polym. Commun.* **1991**, *32*, 390.
42. Kim, S. H.; Dugger, M. T.; Mittal, K. L. Adhesion Aspects in MEMS/NEMS; CRC Press: Boston, **2010**, pp. 377–309.
43. Effati, E.; Pourabbas, B. *Powder Technol.* **2012**, *219*, 276.